Reprinted with permission from Journal of Applied Physics, 99, 2, (2006), pp. 3530-3536.
Copyright 2006, American Institute of Physics.

Phase formation between lead-free Sn–Ag–Cu solder and Ni(P)/Au finishes

V. Vuorinen, T. Laurila, H. Yu, and J. K. Kivilahti[a)]
Laboratory of Electronics Production Technology, Helsinki University of Technology, P.O. Box 3000, 02150 Espoo, Finland

(Received 16 May 2005; accepted 15 December 2005; published online 31 January 2006)

The interfacial reactions of near-eutectic Sn–Ag–Cu solder with Ni(P)/Au metal finishes on printed wiring boards as well as in component under bump metallizations have been investigated in this work. With the help of the scanning electron microscopy and transmission electron microscopy it was discovered that the first phase to form was the metastable nanocrystalline ternary NiSnP layer that provided the substrate for the subsequent formation of $(Cu,Ni)_6Sn_5$. During cooling or in the subsequent reflows the metastable NiSnP layer partially transformed into the columnar Ni_3P. In this transformation Sn atoms and impurities, which do not dissolve into the Ni_3P, diffuse towards the remaining NiSnP layer. When the specimens are further annealed in solid state at 170 °C the Ni_3P phase transforms into Ni_5P_2 implying that some more Ni has diffused towards the solder. However, when Ni(P)/Au finishes with a higher P content were used, only the ternary NiSnP layer was observed. Based on the mass balance and available thermodynamic data on the Sn–P–Ni system the evolution of the observed microstructures in the reactions between the solder and Ni(P)/Au finishes is discussed. © *2006 American Institute of Physics*. [DOI: 10.1063/1.2166647]

I. INTRODUCTION

During recent years Ni/Au coatings have been extensively used in high-density component assemblies as a surface finish on printed wiring boards (PWBs) because they have many advantages over other surface finishes such as hot air solder leveling (HASL) Sn–Pb finishes. Ni/Au coatings provide desired flat and uniform pad surface and they maintain good wettability, even after multiple reflows. Furthermore, Ni/Au coatings provide higher mechanical strength and resistance against thermal fatigue of lead-free solder interconnections than can be achieved when using organic solder preservatives (OSPs) on Cu pads.[1] Moreover, as an insulating material OSP has a disadvantage when connectors are assembled on the same board. Finally, nickel acts as a diffusion barrier layer between Sn-based solders and copper conductors and prevents the underlying copper from reacting with Sn.[2]

On the other hand, reliability problems have been reported when using Ni/Au coatings with Sn-based solders. Problems have appeared, especially when using the electroless Ni/immersion Au finish.[3–11] During the electroless coating process Ni is deposited on Cu together with phosphorus, because hypophosphite is used as a reducing agent in plating baths. It is the presence of phosphorus in the surface finish layers that has been observed to be associated with the above-mentioned reliability problems. Although the wetting occurs properly and the chemical reaction between Sn and Ni is evident, the interfacial strength is not adequate. The weakest interfacial reaction product readily fractures under mechanical stress even during cooling from soldering temperatures and leaves behind an open circuit. The root cause for the brittle fracture has been discussed in many papers dealing with the reactions between electroless Ni and SnPb solders as well as lead-free solders, mainly near-eutectic SnAgCu.[12–22] However, the formation mechanism of the interfacial reaction products that causes the reliability problem has not yet been identified with certainty. It has been claimed that the segregation of phosphorus on the PWB side of the fractured surface is responsible for the failure at the Ni_3Sn_4/Ni(P) interface in as-reflowed ball grid array (BGA) solder interconnections.[7] Jang *et al.*[23] detected phosphorous enrichment in the Si/SiO_2/Al/Ni(P)/63Sn37Pb multilayer structure after reflow and suggested that the formation mechanism of the interfacial reaction layers is related to the so-called solder-assisted crystallization. The mechanism is based on the preferential dissolution of Ni from the Ni(P) layer, which leads to an increase in the phosphorous content of the upper part of the Ni(P) layer and the subsequent formation of Ni_3P.[23] There are also suggestions that the brittle fracture is related to the redeposition of $AuSn_4$ at the interface after high-temperature annealing.[7,11,23–27] However, this can only happen if the amount of Au (i.e., the thickness of the Au coating) exceeds its solubility in β-Sn at the annealing temperature. In particular, if the intermetallic compound (IMC) formed at the interface after reflow is Cu_6Sn_5 or $(Cu,Ni)_6Sn_5$ (in the case of Cu-bearing solders), the latter explanation is not plausible. We have shown previously that the local equilibrium between the $AuSn_4$ and the $(Cu,Au)_6Sn_5$ (as well as with Sn) is possible only if the amount of Au in $(Cu,Au)_6Sn_5$ is close to 20 at. %.[28] Thus, with very thin Au layers used in practice, the redeposition of $AuSn_4$ should not occur, since it is highly unlikely that such high Au concentrations inside $(Cu,Au)_6Sn_5$ could be realized.

Investigations of the reliability of lead-free electronics have recently been intensified much due to the EU legisla-

[a)]Author to whom correspondence should be addressed; electronic mail: jorma.kivilahti@hut.fi

 © 2006 American Institute of Physics

Downloaded 17 Feb 2006 to 130.233.166.170. Redistribution subject to AIP license or copyright, see http://jap.aip.org/jap/copyright.jsp

tion, which ban the usage of lead in consumer electronic products by the first of July 2006. Although it has been demonstrated that lead-free soldering is technologically feasible and has some distinct advantages over Sn–Pb soldering, there are technical issues that remain to be solved. One of the main issues affecting the reliability is the metallurgical compatibility of various board finishes and component metallizations with lead-free solder fillers. Therefore, the purpose of the present work is to study the interfacial reactions between near-eutectic Sn–Ag–Cu solder and Ni(P)/Au finishes both experimentally and theoretically.

II. EXPERIMENTAL PROCEDURE

A. Soldering

The PWB's (Aspocomp Co.) surface finish on Cu was composed of a 2 μm electroless Ni(P) c oating and a 0.02 μm Au coating. The Ni(P) layer contained about 16 at. % (9 wt %) P. The fresh boards were reflow soldered with Sn4.1Ag1.3Cu at. % (Sn3.8Ag0.7Cu wt %) solder paste (Multicore Solders) and subsequently aged under the same reflow profile four times. The reflow soldering was performed under air atmosphere in a Heraus Ewos 5.1 production furnace containing five heating zones and one cooling zone. The peak temperature on the printed wiring boards was measured to be 240 °C (with ECD Super M.O.L.E. Gold). The duration of the spike zone of the reflow profile was about 50 s. Further, some joints were also annealed at 170 °C for different periods of time (up to 640 h). The same PWBs and solder pastes were used to assemble commercial SnAgCu-bumped wafer-level chip scale package (WL-CSP) components with different electroless Ni(P) UBMs (National Semiconductor Corp.) in order to investigate the effect of phosphorous content on the interfacial reactions. The Ni(P) layer contained about 30 at. % (~18 wt %) P. The extended reflow times (up to 20 min) at 250 °C were used to enhance the growth of the interfacial reaction products.

B. Sample preparation for microanalysis

Cross sections of the as-soldered and aged joints were prepared with the standard metallographic methods. Some samples were slightly etched in a dilute solution of CH_3OH+HCL. The microstructures of the interfacial regions were studied by means of an optical light microscope (Olympus BX60) and scanning electron microscope (SEM, JEOL 6335F). The distributions of the elements at the interfacial regions were analyzed with the help of an energy-dispersive x-ray spectroscope (EDS, Oxford, INCA). The interfacial reaction products were also characterized with transmission electron microscope (TEM, JEOL 2000FX) operated at 200 kV and equipped with microanalyzator. Some high-resolution micrographs were also taken at 400 kV. The sample preparation was carried out with conventional Ar-ion milling such as focused ion beam (FIB), and was found to be too aggressive. This enabled us to minimize artifacts from the sample preparation.

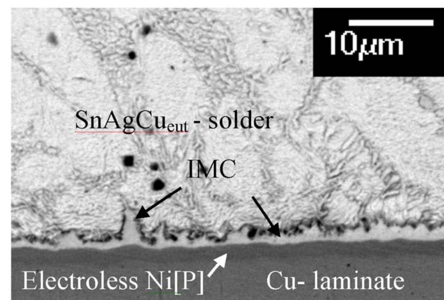

FIG. 1. Backscattered SEM image of a sample that has been reflowed five times.

III. RESULTS AND DISCUSSION

Figure 1 shows the IMC layer between the NiP and near-eutectic solder from the sample that has been reflowed four times after the assembly reflow. The point analysis taken from the interfacial IMC layer gives 40 at. % Cu, 15 at. % Ni, and 45 at. % Sn indicating that the IMC is $(Cu,Ni)_6Sn_5$, where Ni is dissolved into the Cu sublattice. Similar results have been reported in several papers dealing with the Sn–Cu–Ni system.[29–32] However, Hwang *et al.* have suggested that this phase could be Ni_3Sn_2, where Cu is dissolved into the Ni sublattice.[33] As both phases have the same NiAs structure with similar lattice parameters the analysis is difficult to confirm even with TEM. On the other hand, considering the relatively low solubility of Cu in $(Ni,Cu)_3Sn_2$ (Refs. 34 and 35) it is more likely that the intermetallic layer is $(Cu,Ni)_6Sn_5$. A TEM micrograph from the sample that has been reflowed five times given in Fig. 2(a) exhibits that another phase has precipitated out from$(Cu,Ni)_6Sn_5$. The elemental maps [see Figs. 2(b)–2(e)] reveal that the phase contains Ni and Sn and a small amount of Cu. The two phases that can be in local equilibrium with $(Cu,Ni)_6Sn_5$ are $(Ni,Cu)_3Sn_4$ and $(Ni,Cu)_3Sn_2$.[35] With the help of the selected area diffraction (SAD) pattern [see Fig. 2(f)] it can be confirmed that this phase is $(Ni,Cu)_3Sn_4$ having the monoclinic structure. The presence of $(Ni,Cu)_3Sn_4$ crystals inside $(Cu,Ni)_6Sn_5$ is related to the formation mechanism of the IMC layer and has been discussed elsewhere.[36,37]

Between the IMC and Ni(P) layers a thin (less than 0.5 μm) dark layer can also be seen (Fig. 3) already after the assembly reflow meaning that the layers form fast. In fact, one can distinguish even two layers: the thicker one (dark) and on the top of that a very thin layer (light gray). The contrast difference in the backscattered image indicates that the top layer contains heavier elements than the lower one. According to the point analysis the lower dark layer seems to contain more P than the adjacent layers. Figure 4(a) taken from the sample that has been reflowed five times shows a bright-field TEM image (tilted 90° clockwise) from the IMC and phosphorous-enriched areas, together with the line scan [Fig. 4(b)]. From the TEM micrograph it is confirmed that the P-rich phase between the electroless Ni(P) and the $(Cu,Ni)_6Sn_5$ is not a single reaction layer but is composed of two layers, as indicated also by the SEM micrograph (Fig. 3). The layer next to the electroless Ni(P) is a crystalline nickel-phosphide containing more P than the initial electro-

Downloaded 17 Feb 2006 to 130.233.166.170. Redistribution subject to AIP license or copyright, see http://jap.aip.org/jap/copyright.jsp

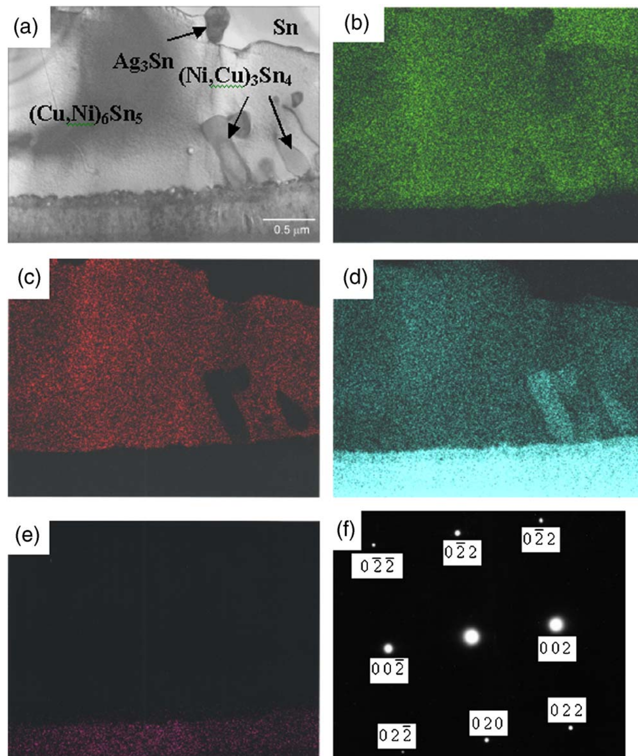

FIG. 2. (a) Bright-field TEM image of the interfacial region in the sample that has been reflowed five times. (b) Sn x-ray map, (c) Cu x-ray map, (d) Ni x-ray map, (e) P x-ray map from the same area, and (f) diffraction pattern taken from the $(Ni,Cu)_3Sn_4$ phase.

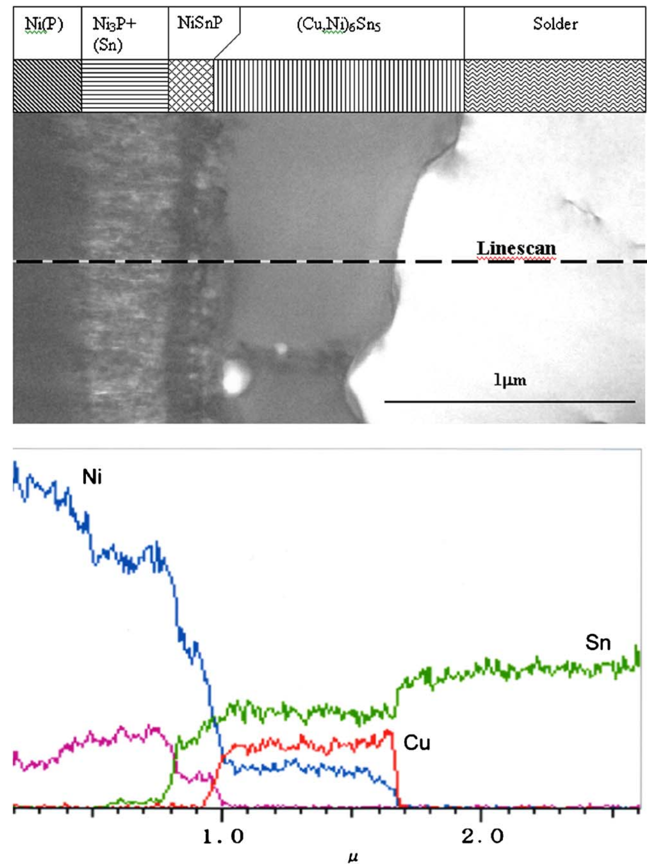

FIG. 4. (a) Bright-field image taken from the IMC and phosphorous-enriched regions in the sample that has been reflowed five times. (b) Line scan presenting the distribution of Ni, P, Sn, and Cu across the reaction zone [depicted with a dotted line in Fig 4(a)].

less Ni(P). Both the line scan and the electron-diffraction pattern (see Fig. 5) point out that this phase is Ni_3P. This phase was observed first by Jang *et al.* when studying $Si/SiO_2/Al/Ni(P)/63Sn37Pb$ multilayer structure after the reflow.[23] As shown in Fig. 5 the crystalline Ni_3P next to the original Ni(P) coating has a columnar structure in which some organic impurities seem to be concentrated between the columns. In addition, some Sn can be observed between the Ni_3P columns—close to the ternary layer being composed of Ni, Sn, and P.

On the basis of the line scan the composition of the NiSnP phase is estimated to be 55 at. % Ni, 35 at. % Sn, and 10 at. % P. As it can be seen from the selected area diffraction pattern (Fig. 5) this layer has a nanocrystalline structure. It is unlikely that this phase is Ni_2SnP (Ref. 38) or Ni_3SnP (Refs. 21 and 33) reported earlier. The determination of the crystal structure of this phase unambiguously is very difficult due to the fact that the diffraction pattern taken from such a thin phase (less than 100 nm) includes diffraction spots from the adjacent crystalline phases. The ternary NiSnP layer contains numerous small defects that have a porelike appearance. It is likely that these structural defects assist the crack propagation in the layer and thus make interconnections to behave in a brittle manner. These "pores" are not artifacts generated during the thinning process, because they were readily observed before the thinning. The pores were also observed by Jeon *et al.*[39] in $Ni(P)/(SnPb)_{eut}$ reaction products and they claim that they are Kirkendall voids. It is difficult to accept that Kirkendall voids could form in the reaction layers in such a short time. Moreover, we did not observe any detectable change in the number or size of these pores in the ternary NiSnP layer when comparing the samples which were either reflow soldered five times or annealed at 170 °C for 64 h after the assembly reflow (see Fig. 6). Therefore, it is unlikely that they are Kirkendall voids. In fact, high-resolution phase contrast images, shown in Fig. 7, point out that the pores contain organic material that most probably originates from the Ni(P) plating bath.

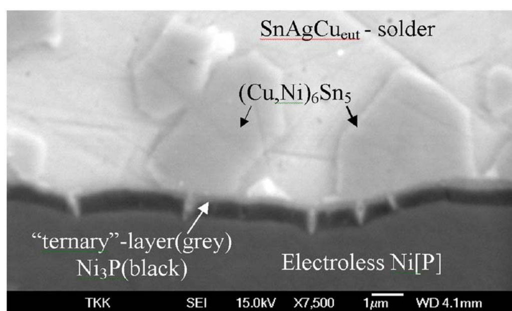

FIG. 3. Secondary SEM image revealing the presence of the dark P-rich layer after the first reflow.

When attempting to rationalize the formation of the observed reaction structures—also reported in other recent publications[33,38,39]—with the help of the solder-assisted crystallization approach we encountered several problems which most probably are due to the fact that the system studied by Jang *et al.*[23] is metallurgically different from ours. In particu-

Downloaded 17 Feb 2006 to 130.233.166.170. Redistribution subject to AIP license or copyright, see http://jap.aip.org/jap/copyright.jsp

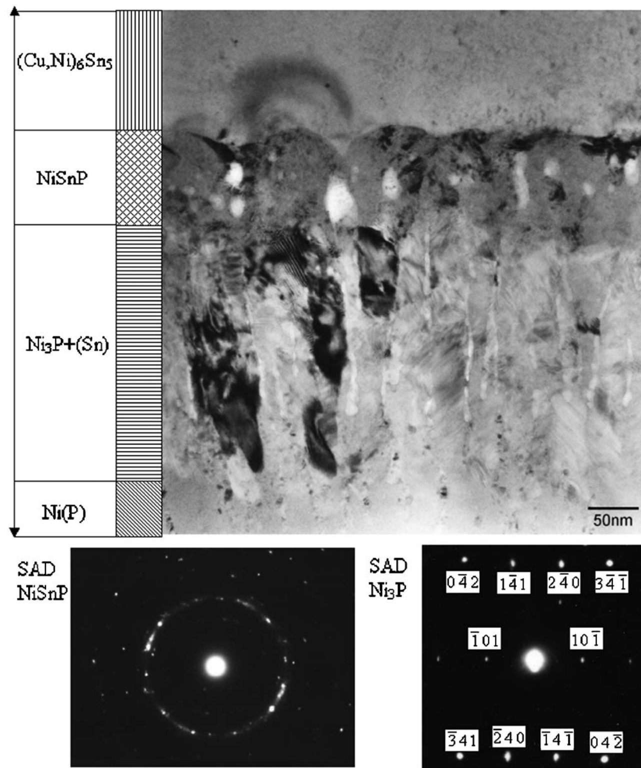

FIG. 5. Bright-field image from the reaction zone together with the diffraction patterns taken from the NiSnP and Ni_3P layers.

lar, the presence of a nanocrystalline NiSnP layer between the Ni_3P and IMC complicates the situation. Firstly, to obtain such a high Ni content as found in the NiSnP layer requires substantial Ni dissolution. However, as both the stable and metastable solubilities of Ni in liquid Sn or eutectic SnAgCu alloy—and therefore also the dissolution rates—are very small, it is hard to accept that so high amounts of Ni could be incorporated in the ternary layer. Secondly, what is even more problematic is that in the solder-assisted crystallization approach only Ni dissolves from the amorphous Ni(P) coating leaving a phosphorous-rich layer behind. This, in turn, requires the solid-state diffusion of Ni inside the Ni(P) coating so that the Ni atoms can reach the Ni(P)/solder interface. This can hardly take place in such a short period of time. Therefore, in our opinion the solder-assisted crystallization approach cannot be applied to our system.

In order to explain the formation of above-mentioned reaction products more quantitatively the thermodynamic description of the quaternary Sn–Ni–P–Cu system is needed for the reasons explained earlier.[36] Unfortunately, there are not enough reliable data on the quaternary system as would be required for its critical thermodynamic assessment. However, it is still plausible to analyze the reactions by making use of the available experimental phase diagram information on the lower-order systems. To explain the microstructures generated in the reactions between the amorphous Ni(P) coating and liquid near-eutectic Sn–Ag–Cu solder we utilize primarily the binary phase diagrams Sn–P and Ni–P (Ref. 40) as well as thermodynamic evaluations concerning the stability of ternary Sn–P–Ni liquids.[41]

The successive reactions between Ni(P) and liquid

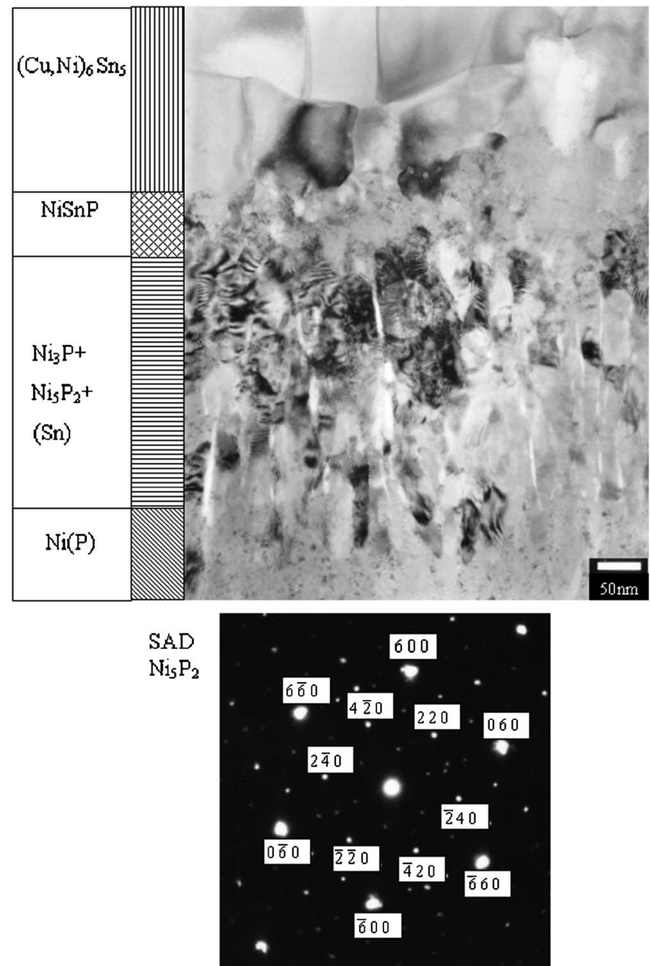

FIG. 6. Bright-field image from the reaction zone in the sample that has been annealed at 170 °C for 64 h after the assembly reflow as well as the diffraction pattern taken from the Ni_5P_2 phase.

SnAgCu solder alloy start with instant dissolution of a thin (flash) Au layer, which is followed by the dissolution of Ni and P. Because of the supersaturation of phosphorus in the Sn-rich liquid a thin layer of new liquid (L_2) is formed between the solid Ni(P) and the bulk liquid solder (L_1). This argument is supported by the presence of the liquid miscibility gap in the binary Sn–P system that extends to lower temperatures as a metastable miscibility gap.[40] On the basis of thermodynamics, it is evident that the binary miscibility gap extends to the ternary Sn–P–Ni system. In fact, accord-

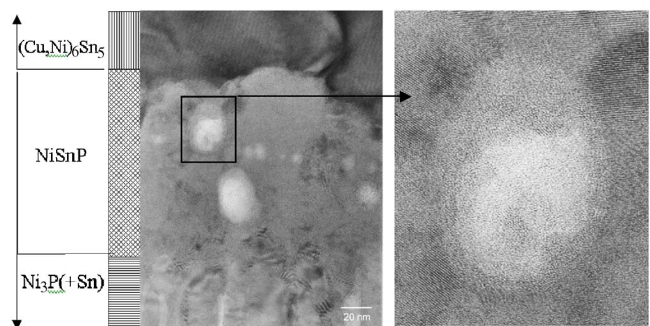

FIG. 7. High-resolution phase contrast image of the organic particles in the nanocrystalline Ni–Sn–P layer.

Downloaded 17 Feb 2006 to 130.233.166.170. Redistribution subject to AIP license or copyright, see http://jap.aip.org/jap/copyright.jsp

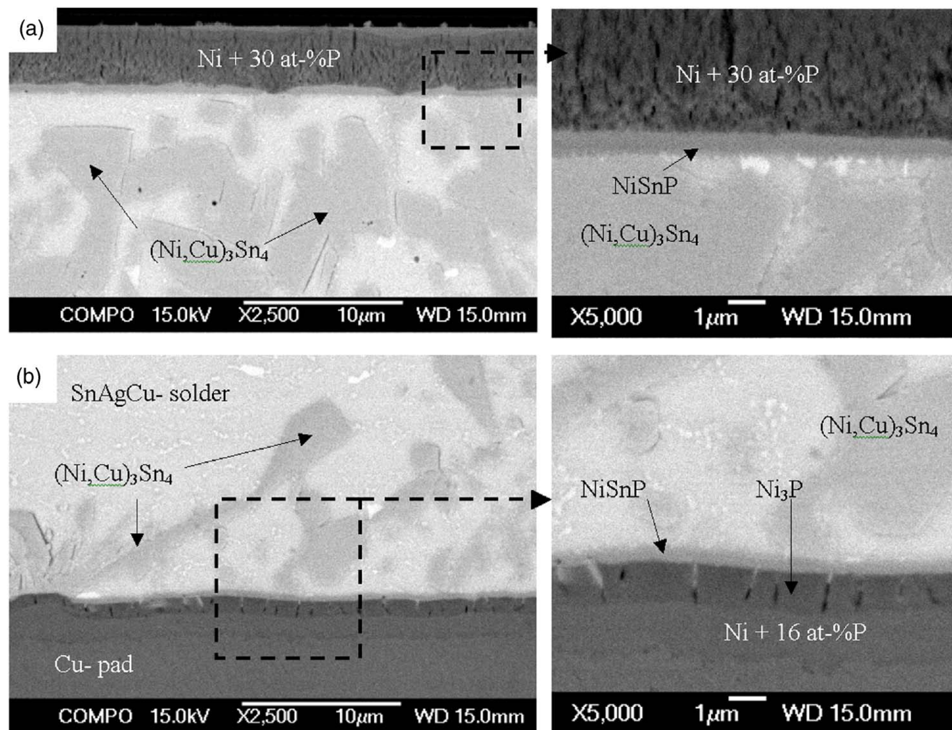

FIG. 8. Backscattered SEM images from the samples that have been annealed for 5 min at 250 °C: (a) the component side, where the P concentration in Ni(P) is about 30 at. %, and (b) the PWB side, where the P concentration in Ni(P) is about 16 at. %.

ing to our calculations the metastable miscibility gap seems to be strongly stabilized by dissolved Ni. Because the two liquids are in local equilibrium with each other and the L_2 with the Ni(P) substrate, Ni, P, and Sn will distribute between the liquids in such a manner that the liquid L_2 contains large amounts of Ni and P and a small amount of Sn, while the Sn-rich liquid L_1 has some Ni and a small amount of P. On the basis of the mass balance calculations, the average composition of the L_2 was estimated to be about 70 at. % Ni, 10 at. % Sn, and 20 at. % P. Because of the high Ni content, the liquid L_2 must be unstable at these low temperatures and therefore it turns rapidly into the ternary NiSnP layer providing a solid substrate for the $(Cu,Ni)_6Sn_5$ to nucleate and grow. After this the reactions take place essentially in the solid state.

During cooling from the upper reflow temperature or during successive reflows the NiSnP layer transforms partially into a more stable crystalline compound Ni_3P with a columnar structure. During the transformation the extra atoms not being used in the formation of Ni_3P are rejected to the ternary NiSnP layer. In addition to P and Sn organic additives that are always present in electroless Ni(P) coatings also precipitate out at the interfaces between the columnar Ni_3P crystals, as well as in the NiSnP phase, where they are revealed as numerous small pores, as shown in Fig. 7. The fact that they are organic impurity particles has been confirmed with the high-resolution transmission electron microscopy (Fig. 7). Therefore, the Kirkendall voids reported earlier[33,38] may, in fact, be organic impurity particles. Also the white stripes between the columnar Ni_3P crystals in Fig. 5, as observed also by Matsuki *et al.*,[38] seem to be organic material, because their bright-field contrast does not change by tilting the specimen. When the specimens were annealed in solid state at 170 °C the Ni_3P phase transforms into Ni_5P_2 implying thatsome more Ni have diffused towards the solder and the P concentration of this layer has increased accordingly.

It is interesting to find out that when the P content of the electroless Ni(P) coating is high enough, the formation of Ni_3P seems to be suppressed. This is shown in Fig. 8(a), where Ni(P) with 30 at. % P has reacted with the near-eutectic Sn–Ag–Cu solder at 250 °C for 5 min. Only the ternary NiSnP layer is visible between the electroless Ni(P) coating and the solder. Furthermore, as the time above the liquidus is now longer (5 min) more Ni (and P) is dissolved into the solder and the $(Cu,Ni)_6Sn_5$ has transformed into $(Ni,Cu)_3Sn_4$ as a result of the limited supply of Cu. Figure 8(b) shows clearly the dark Ni_3P layer in the reaction zone in the PWB side, where the P concentration of the electroless Ni(P) is about 16 at. %. The suppression of the formation of Ni_3P when using electroless Ni with a high P concentration is, in our opinion, due to the increase of P concentration in the NiSnP layer, which is related to the shape of liquid miscibility gap. According to our extrapolated metastable ternary Sn–Ni–P phase diagram, the miscibility gap extends to the ternary system in such a manner that the P concentration of liquid L_1 always remains low while the P content in liquid L_2 may vary significantly. Calculations suggest that most of the dissolved P atoms stay in the liquid L_2 and higher P content in the original Ni(P) results in higher P content in the NiSnP layer.

What has been stated above leads to the situation, where the P content of L_2 can be quite high when the Ni(P) substrate has high P concentration. Therefore, the P content of the resulting NiSnP phase should be also higher than, for example, in the previous case discussed above. We expect that the higher phosphorus content will further stabilize the NiSnP phase at the expense of the crystalline Ni_3P, mainly

Downloaded 17 Feb 2006 to 130.233.166.170. Redistribution subject to AIP license or copyright, see http://jap.aip.org/jap/copyright.jsp

for the following reason. It is known that the temperature of crystallization—and also the glass transition temperature—of an amorphous phase is usually lower close to the eutectic point (19 at. % P in the Ni–P system) than near intermediate compounds or end elements.[42] Therefore, we can expect that an increase in the P content of the NiSnP layer will also increase its crystallization temperature, as the composition is shifted further away from the eutectic point. Further support for the effect of P on the stability of amorphous structures can be found from the literature, where it has been widely documented that when processing diffusion barriers for thin-film applications amorphous structures are frequently realized by alloying elements such as B, C, N, Si, and P with transition metals.[43]

IV. CONCLUSION

The interfacial reactions between the Sn–Ag–Cu solder and Ni(P)/Au coatings on printed wiring boards have been investigated and a reaction mechanism was proposed. Immediately after the solder has melted Au, Ni, and P start dissolving rapidly into the liquid solder, which—due to the existence metastable liquid miscibility gap in the Sn–P–Ni system—is divided into Sn-rich liquid (L_1) and (Ni,P)-rich liquid (L_2). Because of high Ni content the L_2 is unstable and it transits into the nanocrystalline NiSnP, which provides the substrate for the formation of the $(Cu,Ni)_6Sn_5$. Subsequently the metastable NiSnP layer starts to transform into the columnar Ni_3P. In this transformation Sn atoms and impurities, which do not dissolve into the Ni_3P diffuse towards the remaining NiSnP layer. The impurities in this ternary layer are revealed as numerous small "pores" detected with the high-resolution transmission electron microscopy. What is of special interest is that when the P content of the Ni(P) layer is increased, only the NiSnP layer is formed in the assembly reflow within the resolution limits of SEM. The total thickness of the reaction layers does not change considerably during additional reflows. On the other hand, when the specimens were annealed in solid state at 170 °C the Ni_3P phase transforms into Ni_5P_2 implying that some more Ni has diffused towards the solder.

ACKNOWLEDGMENTS

The authors greatly acknowledge Dr. Kejun Zeng and Toni Mattila for useful discussions on the interfacial reactions. The authors are indebted to Yoshioka from JEOL Ltd. for his help in transmission electron microscopy.

[1]T. T. Mattila, V. Vuorinen, and J. K. Kivilahti, J. Mater. Res. **19**, 3214 (2004).
[2]P. G. Kim, J. W. Jang, T. Y. Lee, and K. N. Tu, J. Appl. Phys. **86**, 6746 (1999).
[3]F. D. B. Houghton, Circuit World **26**, 10 (2000).
[4]V. F. Hribar, J. L. Bauer, and T. P. O'Donnell, *Proceedings of the Third International SAMPE Electronics Conference*, 20–22 June 1989, Los Angeles, CA (Society for the Advancement of Material and Process Engineering, Covina, CA, 1989), pp. 1187–1199.
[5]K. Puttlitz, IEEE Trans. Compon., Hybrids, Manuf. Technol. **13**, 647 (1990).
[6]E. Bradley and K. Banerji, *Proceedings of the 45th Electronic Components and Technology Conference*, 21–24 May 1995, Las Vegas, NV (IEEE, Piscataway, 1995), pp. 1028–1038.
[7]Z. Mei, P. Callery, D. Fisher, F. Hua, and J. Glazer, *Proceedings of the Pacific Rim/ASME International Intersociety Electronic and Photonic Packaging Conference, Advances in Electronic Packaging 1997* (ASME, New York, 1997), Vol. 2, pp. 1543–1550.
[8]R. Ghaffarian, *Proceedings of the Surface Mount International Conference and Exposition '98*, SMTA, Edina, 1998 (Surface Mount International, San Jose, 1998), pp. 59–69.
[9]R. W. Johnson, V. Wang, and M. Palmer, *Proceedings of the Surface Mount International Conference and Exposition '98*, SMTA, Edina, 1998 (Surface Mount International, San Jose, 1998), pp. 681–686.
[10]Z. Mei, M. Kaufmann, A. Eslambolchi, and P. Johnson, *Proceedings of the 48th Electronic Components and Technology Conference*, 25–28 May 1998, Seattle, WA (IEEE, Piscataway, 1998), pp. 952–961.
[11]Z. Mei, P. Johnson, M. Kaufmann, and A. Eslambolchi, *Proceedings of the 49th Electronic Components and Technology Conference*, 1–4 June 1999, San Diego, CA (IEEE, Piscataway, 1999), pp. 125–134.
[12]J.-W. Yoon, S.-W. Kim, and S.-B. Jung, J. Alloys Compd. **385**, 192 (2004).
[13]S. J. Hang, H. J. Kao, and C. Y. Liu, J. Electron. Mater. **33**, 1130 (2004).
[14]S.-W. Kim, J.-W. Yoon, and S.-B. Jung, J. Electron. Mater. **33**, 1182 (2004).
[15]M. He, Z. Chen, and G. Qi, Acta Mater. **52**, 2047 (2004).
[16]M. He, Z. Chen, G. Qi, C. C. Wong, and S. G. Mhaisalkar, Thin Solid Films **462–463**, 363 (2004).
[17]M. He, A. Kumar, P. T. Yeo, G. J. Qi, and Z. Chen, Thin Solid Films **462–463**, 387 (2004).
[18]M. O. Alam, Y. C. Chan, and K. N. Tu, J. Appl. Phys. **94**, 4108 (2003).
[19]B.-L. Young, J.-G. Duh, and G.-Y. Jang, J. Electron. Mater. **32**, 1463 (2003).
[20]M. O. Alam, Y. C. Chan, and K. C. Hung, Microelectron. Reliab. **42**, 1065 (2002).
[21]Y.-D. Jeon, K.-W. Paik, K.-S. Bok, W.-S. Choi, and C.-L. Cho, J. Electron. Mater. **31**, 520 (2002).
[22]P. L. Liu and J. K. Shang, Metall. Mater. Trans. A **31A**, 2867 (2000).
[23]J. W. Jang, P. G. Kim, K. N. Tu, D. R. Frear, and P. Thompson, J. Appl. Phys. **85**, 8456 (1999).
[24]A. M. Minor and J. W. Morris, Metall. Mater. Trans. A **31A**, 798 (2000).
[25]R. Erich, R. J. Coyle, G. M. Wenger, and A. Primavera, *Proceedings of the 24th IEEE/CPMT International Electronics Manufacturing Technology Symposium*, 18–19 October 1999, Austin (IEEE, Piscataway, 1999), pp. 16–22.
[26]S. C. Hung, P. J. Zheng, S. C. Lee, and J. J. Lee, *Proceedings of the 24th IEEE/CPMT International Electronics Manufacturing Technology Symposium*, 18–19 October 1999, Austin (IEEE, Piscataway, 1999), pp. 7–15.
[27]A. Zribi *et al.*, *Proceedings of the 49th Electronic Components and Technology Conference*, 1–4 June 1999, San Diego, CA (IEEE, Piscataway, 1999), pp. 451–457.
[28]T. Laurila, V. Vuorinen, T. Mattila, and J. K. Kivilahti, J. Electron. Mater. **34**, 103 (2005).
[29]S.-W. Chen, S.-H. Wu, and S.-W. Lee, J. Electron. Mater. **32**, 1188 (2003).
[30]C. E. Ho, R. Y. Tsai, Y. L. Lin, and C. R. Kao, J. Electron. Mater. **31**, 584 (2002).
[31]G. Ghosh, Acta Mater. **49**, 2609 (2002).
[32]G. Ghosh, J. Electron. Mater. **33**, 229 (2004).
[33]C. W. Hwang, K. Suganuma, M. Kiso, and S. Hashimoto, J. Mater. Res. **18**, 2540 (2003).
[34]P. Oberndorff, Ph.D. thesis, Eindhoven University of Technology, 2001.
[35]C.-H. Lin, S.-W. Chen, and C.-H. Wang, J. Electron. Mater. **31**, 907 (2002).
[36]T. Laurila, V. Vuorinen, and J. K. Kivilahti, Mater. Sci. Eng., R. **R49**, 1 (2005).
[37]V. Vuorinen and J. K. Kivilahti (unpublished).
[38]H. Matsuki, H. Ibuka, and H. Saka, Sci. Technol. Adv. Mater. **3**, 261 (2002).
[39]Y.-D. Jeon, K.-W. Paik, K.-S. Bok, W.-S. Choi, and C.-L. Cho, *Proceedings of the 51st Electronic Components and Technology Conference, 2001*, 29 May–1 June 2001 (IEEE, Piscataway, 2001), pp. 1326–1332.
[40]T. Massalski, *Binary Alloy Phase Diagrams* (ASM, Materials Park, OH, 1996).
[41]IPMA, *The Thermodynamic Databank for Interconnection and Packaging Materials*, Helsinki University of Technology, Helsinki, 2004.
[42]W. J. Johnson, Prog. Mater. Sci. **30**, 81 (1986).
[43]M.-A. Nicolet, in *Diffusion in Amorphous Materials*, edited by H. Jain and D. Gupta (TMS, Warrendale, 1994), pp. 225–234.

Downloaded 17 Feb 2006 to 130.233.166.170. Redistribution subject to AIP license or copyright, see http://jap.aip.org/jap/copyright.jsp